LAWS OF NONSTEADY MIXING WITH A REDUCTION IN THE RATE OF FLOW OF A HEAT CARRIER IN A BUNDLE OF COILED TUBES

B. V. Dztybenko, L. A. Ashmantas, and A. B. Bagdonavichyus

UDC 621.564-71:536.423

Laws are established for the occurrence of nonsteady heat- and mass-transfer processes and generalizing relations are proposed to calculate the effective nonsteady diffusion coefficients in an oval bundle of coiled tubes.

Several investigations [2-6] have examined nonsteady heat- and mass-transfer processes in heat exchangers with coiled tubes [1]. However, these studies were conducted only for the cases of abrupt and smooth changes in thermal load over time. At the same time, to ensure the fitness of an exchanger for service, it is necessary to also have data to calculate transient regimes of its operation under conditions of a change in the flow rate of the heat carrier. The authors of [7] proposed relations to determine the effective nonsteady diffusion coefficients with an increase in heat-carrier flow rate in a bundle of coiled tubes. These relations made it possible to close the system of equations and calculate the temperature field in the bundle for this type of transience. The laws governing heat and mass transfer in this case were also determined. It turned out that with an increase in the rate of flow of the heat carrier, the effective diffusion coefficient K_n initially decreases sharply relative to its quasisteady value K_{qs}. Then the coefficient K_n increases smoothly over time and approaches K_{qs} [7]. These laws were established with a constant thermal load on the tubes of the bundle during the experiment. In fact, an increase in the flow rate of the heat carrier over time in this case leads to a reduction in the mean-mass temperature of the coolant and to restructuring of the temperature fields in cross sections of the bundle, analogously to the character of change in the temperature fields of the carrier with a reduction in the thermal load and a constant heat-carrier flow rate [5]. The cooling of the walls on the tubes with an increase in flow rate and a constant thermal load leads to the liberation of additional heat in the flow, a phenomenon connected with the thermal inertia of the tubes. As was noted in [7], this mechanism of nonsteady heat and mass transfer becomes active when the ratio of the flow rate of the heat carrier after the introduction of a perturbation (G_2) to the initial value (G_1) $G_2/G_1 \geq 1.12$, since $T_w(\tau)$ = const with a constant wall temperature over time. According to [8], acceleration of the flow should increase its transport properties. Since wall temperature changed in [7] while the power of the thermal load N = const over time, it turned out that the coefficient K_n remained nearly constant at G_2/G_1 = 1-1.12. The laws established in [7] are valid within the range G_2/G_1 = 1.12-1.77.

Together with the type of transience studied in [7], equally important and common in heat-exchanger operation is the case where the flow rate of the heat carrier decreases sharply over time. However, unitl recently, there has been almost no data on the nonsteady mixing of a heat carrier with a reduction in flow rate.

Here, we report results of an experimental-theoretical study of the nonsteady mixing of a heat carrier with a reduction in flow rate in a bundle of coiled tubes with the number Fr_m = 57. The number Fr_m characterizes the intensity of swirling of the flow in a bundle of coiled tubes and is determined from the expression [1]

$$Fr_m = S^2/(dd_e). \tag{1}$$

The relative pitch of the tubes S/d = 6.1, where d = 12.3 mm is the maximum dimension of the oval profile of the tubes. The tests were conducted on the experimental unit described in [7] with the use of a special device to abruptly change the air flow rate. Such a setup ensured that the system would have low inertia. To collect and analyze experimental data and control the experiment under nonsteady conditions, we used an automatic system based on

Translated from Inzhenerno-Fizicheskii Zhurnal, Vol. 56, No. 1, pp. 5-11, January, 1989. Original article submitted August 24, 1987.

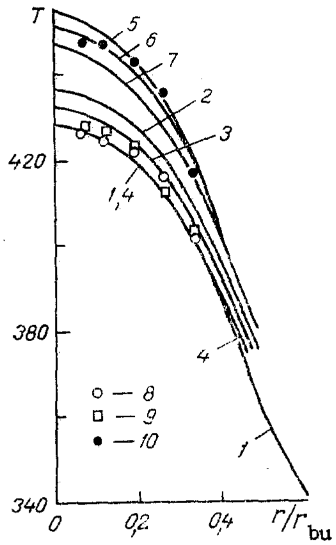

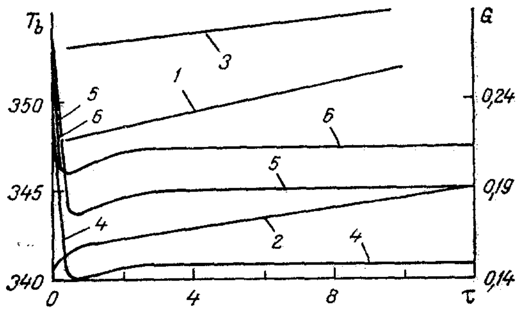

Fig. 1 Fig. 2

Fig. 1. Experimental and theoretical temperature fields of the heat carrier in the outlet section of a bundle of coiled tubes with the number Fr_m = 57 and the ratio G_2/G_1 = 0.605: 1) calculation with G = 0.235 kg/sec, K = 0.09; 2-4) same with τ = 0.8 sec (G = 0.1422), K = 0.09, 0.12, 0.14; 5-7) same with τ = 10 sec (G = 0.148 kg/sec), K = 0.09, 0.10, 0.12; 8-10) experimental data with τ = 0, 0.8, and 10 sec.

Fig. 2. Dependences of flow rate and mean-mass temperature of the heat carrier on time: 1-3) dependences of temperature for G_2/G_1 = 0.605 and N = 6.4 kW, 0.665, and 5.7 kW, 0.765, and 8.6 kW, respectively; 4-6) dependences of flow rate for the same G_2/G_1 and N. T_b, K; τ, sec; G, kg/sec.

measuring-computing complex IVK-2. The effective diffusion coefficient was determined by the method of diffusion from a system of linear heat sources resulting from the heating of a central group of 37 tubes in a 127-tube bundle 0.5 m long by an electric current. The tubes had a thickness of 0.2 mm. The temperature field of the heat carrier at the outlet of the bundle was measured with Chromel–Alumel thermocouples having wires 0.1 mm in diameter. The tests were conducted within the range of flow-rate ratios G_2/G_1 = 0.605-0.765 and the range of thermal loads N = 5.7-8.6 kW. Figure 1 shows experimental temperature fields (in the form of experimental points) for one of the operating regimes of the unit that we used. It was found that due to restructuring the temperature fields over time, the coefficient K_n at first increased sharply and then smoothly decreased, approaching its quasi-steady value. The dimensionless coefficient

$$K_n = D_t/(u d_e), \tag{2}$$

as in [1-7] was determined by comparing the experimental results with heat-carrier temperature fields found by a modification of the least squares method.

The nonsteady temperature fields produced with a sharp reduction in flow rate were calculated by numerically solving a system of equations describing the flow of a two-phase homogeneous medium with a stationary solid phase. Meanwhile, the gasdynamic equations were written in a quasisteady approximation using the experimentally established relation for the flow rate of the heat carrier over time G = G(τ) (Fig. 2). This system has the form [4]:

$$\rho_s c_s \frac{\partial T_s}{\partial \tau} = q_v - \frac{4\alpha m}{(1-m)\,d_e}(T_s - T) + \frac{1}{r}\frac{\partial}{\partial r}\left(r\lambda_{sr}\frac{\partial T_s}{\partial r}\right) + \frac{\partial}{\partial x}\left(\lambda_{sx}\frac{\partial T_s}{\partial x}\right), \tag{3}$$

$$\rho c_p \frac{\partial T}{\partial \tau} + \rho u c_p \frac{\partial T}{\partial x} + \rho v c_p \frac{\partial T}{\partial r} = \frac{4\alpha}{d_e}(T_s - T) + \frac{1}{r}\frac{\partial}{\partial r}\left(r\lambda_e\frac{\partial T}{\partial r}\right) + \frac{\partial}{\partial x}\left(\lambda_e\frac{\partial T}{\partial x}\right), \tag{4}$$

$$\rho u \frac{\partial u}{\partial x} + \rho v \frac{\partial u}{\partial r} = - \frac{\partial p}{\partial x} - \xi \frac{\rho u^2}{2d_e} + \frac{1}{r} \frac{\partial}{\partial r}\left(\rho r \nu_e \frac{\partial u}{\partial r}\right), \tag{5}$$

$$\frac{\partial (\rho u m)}{\partial x} + \frac{1}{r} \frac{\partial}{\partial r}(r\rho v m) = 0, \tag{6}$$

$$p = \rho R T. \tag{7}$$

The following boundary conditions are attached to Eqs. (3)-(7):

a) at the inlet of the bundle (x = 0), the profiles of temperature, velocity, and pressure are known;

b) on the axis of the bundle (r = 0)

$$\partial T_s/\partial r = 0,\ \partial T/\partial r = 0,\ \partial u/\partial r = 0,\ v = 0; \tag{8}$$

c) at the boundary ($r = r_{bu}$)

$$\partial T_s/\partial r = 0,\ \partial T/\partial r = 0,\ \partial u/\partial r = 0,\ v = 0; \tag{9}$$

d) at the outlet ($x = \ell$)

$$\partial T_s/\partial x = 0,\ \partial T/\partial x = 0. \tag{10}$$

The initial distributions $T_s(r,x)$, $T(r,x)$, $u(r,x)$ at $\tau = 0$ were found from the solution of the steady-state problem.

To numerically solve the system of equations, we chose a grid of values of r_i, x_j, τ^ν with the spacings Δr, Δx, and $\Delta\tau$, respectively. The grid subdivides the region of sought functions into M concentric zones over the radius and N layers through the thickness.

We chose the method of variable directions to solve the heat-transfer equations. This method makes it possible to avoid strict limitations on the relationship between the time and space intervals of the grid. In accordance with the chosen model, the heat-transfer equations were split up into two unidimensional equations with respect to the r and x directions. As an example, we present the finite-difference analog of Eq. (3):

$$\begin{aligned} 2\bar{\rho}_s \bar{c}_s \frac{T_{s\,i,j}^{\nu+1/2} - T_{s\,i,j}^{\nu}}{\Delta\tau} &= q_{v\,i,j}^{\nu+1} - \frac{4\alpha m}{(1-m)\,d_e}\left(T_{s\,i,j}^{\nu+1/2} - T_{i,j}^{\nu+1/2}\right) + \\ &+ \frac{\bar{\lambda}_{sr}}{r_i} \frac{T_{s\,i+1,j}^{\nu+1/2} - T_{s\,i-1,j}^{\nu+1/2}}{2\Delta r} + \bar{\lambda}_{sr} \frac{T_{s\,i+1,j}^{\nu+1/2} - 2T_{s\,i,j}^{\nu+1/2} + T_{s\,i-1,j}^{\nu+1/2}}{\Delta r^2} + \\ &+ \bar{\lambda}_{sx} \frac{T_{s\,i,j+1}^{\nu} - 2T_{s\,i,j}^{\nu} + T_{s\,i,j-1}^{\nu}}{\Delta x^2}, \end{aligned} \tag{11}$$

$$\begin{aligned} 2\bar{\rho}_s \bar{c}_s \frac{T_{s\,i,j}^{\nu+1} - T_{s\,i,j}^{\nu+1/2}}{\Delta\tau} &= q_{v\,i,j}^{\nu+1} - \frac{4\alpha m}{(1-m)\,d_e}\left(T_{s\,i,j}^{\nu+1} - T_{i,j}^{\nu+1}\right) + \\ &+ \frac{\bar{\lambda}_{sr}}{r_i} \frac{T_{s\,i+1,j}^{\nu+1/2} - T_{s\,i-1,j}^{\nu+1/2}}{2\Delta r} + \bar{\lambda}_{sr} \frac{T_{s\,i+1,j}^{\nu+1/2} - 2T_{s\,i,j}^{\nu+1/2} + T_{s\,i-1,j}^{\nu+1/2}}{\Delta r^2} + \\ &+ \bar{\lambda}_{sx} \frac{T_{s\,i,j+1}^{\nu+1} - 2T_{s\,i,j}^{\nu+1} + T_{s\,i,j-1}^{\nu+1}}{\Delta x^2}. \end{aligned} \tag{12}$$

We used Simon's substitution to solve equation of motion (5). Inserting the equations of motion $u_{i,j} = \tilde{u}_{i,j} + \tilde{\tilde{u}}_{i,j}(\partial P/\partial x)_j$ into the finite-difference analog, we obtain the following two equalities:

$$\bar{\rho u} \frac{\tilde{u}_{i,j} - \tilde{u}_{i,j-1} - \tilde{\tilde{u}}_{i,j-1}(\partial P/\partial x)_{j-1}}{\Delta x} + \bar{\rho v} \frac{\tilde{u}_{i+1,j} - \tilde{u}_{i-1,j}}{2\Delta r} =$$

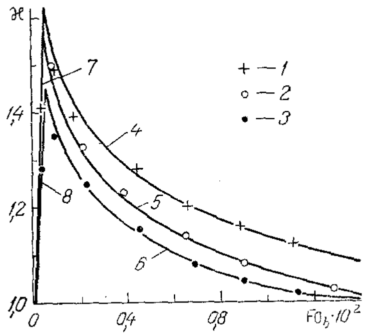

Fig. 3.

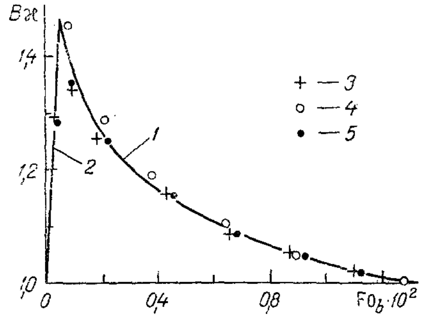

Fig. 4

Fig. 3. Effect of the Froude number and the ratio G_2/G_1 on the relative diffusion coefficient: 1-3) experimental data for the ratios G_2/G_1 = 0.605, 0.655, 0.765; 4-6) Eq. (19) for G_2/G_1 = 0.605, 0.665, 0.765; 7-8) Eq. (18) for G_2/G_1 = 0.605 and 0.765.

Fig. 4. Generalizing dependence of the relative diffusion coefficient on the governing parameters: 1) relation (21); 2) relation (20); 3-5) experimental data for G_2/G_1 = 0.605, 0.665, 0.765, respectively.

$$= -\xi\overline{\rho u}\,\frac{\tilde{u}_{i,j}}{2d_e} + \bar{\rho}\nu_e\,\frac{\tilde{u}_{i+1,j}-\tilde{u}_{i-1,j}}{2r_i\Delta r} + \bar{\rho}\nu_e\,\frac{\tilde{u}_{i+1,j}-2\tilde{u}_{i,j}+\tilde{u}_{i-1,j}}{\Delta r^2}\,, \tag{13}$$

$$\overline{\rho u}\,\frac{\tilde{\tilde{u}}_{i,j}}{\Delta x} + \overline{\rho v}\,\frac{\tilde{\tilde{u}}_{i+1,j}-\tilde{\tilde{u}}_{i-1,j}}{2\Delta r} = -1 - \xi\overline{\rho u}\,\frac{\tilde{\tilde{u}}_{i,j}}{2d_e} + \bar{\rho}\nu_e\,\frac{\tilde{\tilde{u}}_{i+1,j}-\tilde{\tilde{u}}_{i-1,j}}{2r_i\Delta r} + \bar{\rho}\nu_e\,\frac{\tilde{\tilde{u}}_{i+1,j}-2\tilde{\tilde{u}}_{i,j}-\tilde{\tilde{u}}_{i-1,j}}{\Delta r^2}\,, \tag{14}$$

where $\tilde{u}_{i,j}$, $\tilde{\tilde{u}}_{i,j}$ are certain elements of the longitudinal component of the velocity vector.

The pressure gradient is found from the relation

$$\frac{\partial p}{\partial x} = \frac{G - 2\pi m\int_0^{r_{bu}}\rho u\tilde{u} r\,dr}{2\pi m\int_0^{r_{bu}}\rho u\tilde{\tilde{u}} r\,dr}\,. \tag{15}$$

In solving continuity equation (6), we found the transverse component of the velocity vector v on the new grid layer from recursion formulas. Calculations showed that with a constant porosity and a constant hydraulic diameter, the value of v is close to zero.

The solution of the problem was broken down into two successive stages: the "thermal" part of the problem (Eqs. (3) and (4)) and the "gasdynamic" part of the problem (Eqs. (5) and (6)). The solutions of both parts are connected through the equation of state (7). The method allows for the possibility of a change in porosity and hydraulic diameter over both the radius and the height of the bundle.

The above-described method was used to develop an algorithm and write a program in FORTRAN for the BÉSM-6 computer.

The dimensionless effective nonsteady coefficient of eddy diffusion K_n (2) is connected with the effective thermal conductivity $\lambda_e = D_t\rho c_p$ and effective viscosity $\nu_e = D_t$ in Eqs. (4) and (5).

Empirical data on the coefficient K_n was analyzed in dimensionless form

$$\varkappa = K_n/K_{qs} = f(\mathrm{Fo}_b,\ G_2/G_1), \tag{16}$$

where Fo_b is the Fourier criterion, determined from the expression

$$\mathrm{Fo}_b = \frac{\lambda_b\tau}{c_p\rho_b d_{bu}^2}\,, \tag{17}$$

in which the physical properties are determined at the mean-mass temperature of the heat carrier T_b. Figure 2 shows the change in temperature T_b over time for the above-examined operating regimes of the unit. Figure 3 shows the relation (16) for the investigated parameter regimes, where a reduction in the flow rate of the heat carrier (during slowing of the flow) is initially accompanied by a sharp increase in the coefficient K_n (or $\varkappa = K_n/K_{qs}$). Here, the maximum value of χ is reached after 0.46-0.47 sec. The increase in $\varkappa$ from 1 to the maximum value can be described by a linear relation (Fig. 3):

$$\varkappa = 1 + A\,\mathrm{Fo}_b, \tag{18}$$

where A = 927 at G_2/G_1 = 0.765 and A = 1205 at G_2/G_1 = 0.605. Meanwhile, the number Fo_b corresponding to the maximum value of $\varkappa$ is equal to $\mathrm{Fo}_b = (0.512\text{-}0.514)\cdot 10^{-3}$. The value of χ henceforth decreases with time and approaches unity in accordance with the relation

$$\varkappa = A\,\mathrm{Fo}_b^n + C, \tag{19}$$

where

$$A = 3{,}47,\quad n = -0{,}0381,\quad C = -3 \quad \text{for} \quad G_2/G_1 = 0{,}605;$$

$$A = 3{,}548,\quad n = -0{,}0374,\quad C = -3{,}15 \quad \text{for} \quad G_2/G_1 = 0{,}665;$$

$$A = 2{,}57,\quad n = -0{,}0437,\quad C = -2{,}11 \quad \text{for} \quad G_2/G_1 = 0{,}765.$$

Equation (19) is valid for $\mathrm{Fo}_b = 0.514\cdot 10^{-3}\text{-}1.4\cdot 10^{-2}$ and $\varkappa \geq 1$.

The results of study of nonsteady diffusion coefficients with a reduction in the flow rate of the heat carrier can be generalized within the investigated range of G_2/G_1 by single relations: for the numbers $\mathrm{Fo}_b = 0\text{-}0.514\cdot 10^{-3}$

$$\varkappa = [2{,}95\cdot 10^{-4}(G_2/G_1)^{-11,94} + 0{,}993](1 + 927\,\mathrm{Fo}_b), \tag{20}$$

for the numbers $\mathrm{Fo}_b = 0.514\cdot 10^{-3}\text{-}1.4\cdot 10^{-2}$

$$\varkappa = [2{,}95\cdot 10^{-4}(G_2/G_1)^{-11,94} + 0{,}993](2{,}57\,\mathrm{Fo}_b^{-0,0437} - 2{,}11). \tag{21}$$

Figure 4 shows the relations (20) and (21) in the form $B\varkappa = f(\mathrm{Fo}_b)$, where $B = [2.95\cdot 10^{-4}(G_2/G_1)^{-11.94} + 0.933]^{-1}$. The agreement between the experimental and theoretical data in such a representation is good.

Thus, the character of change in the coefficient $\varkappa$ over time with a reduction in the flow rate of the heat carrier and a constant thermal load proved to be similar to the character of change in the coefficient $\varkappa$ in the case of an increase in the thermal load and G = const [2, 3, 6]. At the same time, with a sudden increase in the thermal load, the coefficient K_n may initially exceed the coefficient K_{qs} by a factor of 3-5 [2, 3, 6], while the coefficient $\varkappa$ = 1.63-1.46 with a reduction in the flow rate of the heat carrier G_2/G_1 = 0.605-0.765 and and N = const. Also, the transition from a steady-state regime of operation to an unsteady regime with a reduction in flow rate and N = const occurs at a finite rate in accordance with Eq. (20), while the same transition occurs nearly instantaneously with a sudden increase in thermal load and G = const and could not be determined experimentally in [2, 3, 6]. Such a quantitative difference in the course of the nonsteady heat and mass transfer processes for the above-examined types of transience can be attributed to the fact that with slowing of the flow in the case T_w = const, there should be a decrease in the heat-transfer coefficients [8]. In the case N = const, the wall is heated, its temperature increases, and less heat enters the flow, which leads to a reduction in the coefficient K_n. The effect of the mechanism responsible for reducing the coefficient K_n partially compensates for the effect of the mechanism causing its increase, which leads to the observed dependence of the coefficient $\varkappa$ on the number Fo_b and the ratio G_2/G_1. The effect of the flow-rate ratio G_2/G_1 is expressed both in a change in the rate of attainment of the maximum value of the coefficient $\varkappa_m$ and in the value of $\varkappa_m$. The smaller the ratio G_2/G_1, the greater the value of $\varkappa_m$ and the faster it is reached (Fig. 3).

The above-observed laws governing the nonsteady mixing of a heat carrier with a reduction in its rate of flow are evidence of the need to consider the difference between the nonsteady diffusion coefficients and the quasisteady values of same when calculating temperature fields in a bundle of coiled tubes. The relations proposed for calculating K_n make it possible to close system (3-7) and to perform thermohydraulic calculations for heat exchangers for the above-examined type of transience.

NOTATION

N, Power of thermal load; τ, time; G_1, initial flow rate of heat carrier; G_2, maximum flow rate of heat carrier after introduction of a perturbation into the feed system; m, porosity of the bundle with respect to the heat carrier; K, dimensionless effective diffusion coefficient; D_t, effective diffusion coefficient; u, v, longitudinal and radial velocities; d_e, equivalent diameter of the bundle; Fr_m, criterion characterizing the intensity of swirling of the flow in the bundle of coiled tubes; S, pitch of the tube coiling; d, maximum dimension of tube profile; Fo_b, Fourier criterion; d_{bu}, r_{bu}, diameter and radius of the tube bundle; λ, thermal conductivity; c_p, heat capacity; ρ, density; ξ, hydraulic resistance coefficient; γ, kinematic viscosity; $\varkappa$, relative diffusion coefficient; T, temperature; x, r, longitudinal and radial coordinates. Indices: b, mean-mass; w, wall; n, nonsteady; qs, quasi-steady; m, maximum; e, effective; s, solid phase.

LITERATURE CITED

1. Yu. I. Danilov, B. V. Dzyubenko, G. A. Dreitser, and L. A. Ashmantas, Heat Transfer and Hydrodynamics in Channels of Complex Form [in Russian], Moscow (1986).
2. B. V. Dzyubenko, M. D. Segal', L. A. Ashmantas, and P. A. Urbonas, Izv. Akad. Nauk SSSR, Énerg. Transp., No. 3, 125-133 (1983).
3. B. V. Dzyubenko, L. A. Ashmantas, M. D. Segal', and P. A. Urbonas, Izv. Akad. Nauk SSSR, Énerg. Transp., No. 4, 110-118 (1985).
4. B. V. Dzyubenko, L. A. Ashmantas, and A. B. Bagdonavichyus, Inter-Institute Collection of Scientific Transactions: Current Problems of Hydrodynamics and Heat Transfer in Elements of Power Plants and Cryogenic Technology, Vol. 14, 9-14, Moscow (1985).
5. B. V. Dzyubenko, L. A. Ashmantas, A. B. Bagdonavichyus, and M. D. Segal', Inzh.-Fiz. Zh., 54, No. 4, 533-539 (1988).
6. L. A. Ashmantas, B. V. Dzyubenko, G. A. Dreitser, and M. D. Segal, Int. J. Heat Mass Transfer, 28, No. 4, 867-877 (1985).
7. B. V. Dzyubenko, L. A. Ashmantas, and A. B. Bagdonavichyus, Inzh.-Fiz. Zh., 55, No. 3, 357-363 (1988).
8. É. K. Kalinin, G. A. Dreitser, V. V. Kostyuk, and I. I. Berlin, Methods of Calculating Coupled Heat-Transfer Problems [in Russian], Moscow (1983).

STUDY OF HYDRODYNAMICS AND MASS TRANSFER IN THE FLOW OF OPPOSITELY SWIRLED JETS ABOUT A STABILIZER IN AN ANNULAR CHANNEL

K. Yu. Sokolov, A. G. Tumanovskii,
A. I. Maiorova, A. V. Sudarev,
and E. D. Vinogradov

UDC 532.517.4

Experimental and theoretical methods are used to study the distribution of the velocity components, turbulence intensity, and the concentration of a passive impurity. An analysis is made of the effect of the main geometric parameters on the intensity of transport processes.

At present in the annular combustion chambers of gas-turbine units, combustion takes place in a system of oppositely swirled jets of gaseous and liquid fuel [1].

The results of experimental [1, 2] and theoretical [2] studies of the separation zone after the stabilizer and the available data on the displacement of oppositely swirled jets in an annular channel [3, 4] prove to be inadequate to analyze processes taking place in the

---

F. É. Dzerzhinskii All-Union Scientific-Research Institute of Heat Engineering, Moscow.
Translated from Inzhenerno-Fizicheskii Zhurnal, Vol. 56, No. 1, pp. 12-18, January, 1988. Original article submitted August 10, 1987.

